



A cancer-targetable copolymer containing tyrosine segments for labeling radioactive halogens

Yu Qi, Najun Li*, Qingfeng Xu, Xuewei Xia, Jianfeng Ge, Jianmei Lu*

Key Laboratory of Organic Synthesis of Jiangsu Province, College of Chemistry, Chemical Engineering and Materials Science, Suzhou University, Suzhou, Jiangsu 215123, China

ARTICLE INFO

Article history:

Received 13 July 2010

Received in revised form 12 December 2010

Accepted 13 December 2010

Available online 21 December 2010

Keywords:

Copolymer

Synthesis

Tyrosine

Isotope

Targeting

ABSTRACT

A series of cancer-targetable copolymers containing rhodamine and tyrosine segments were synthesized and further labeled with isotope ^{125}I . Copolymers with different molecular weights (PRTH-1, PRTH-2 and PRTH-3) formed aggregates in water with average diameters of 66 nm, 191 nm and 137 nm, respectively. The cancer cell targeting properties of the copolymers were investigated by comparing BEL-7402 liver cancer cells and L-02 human normal liver cells. The results indicate that their targeting properties are related to the average diameters of the PRTH copolymers that self-assembled in water. PRTH-2 copolymers were selected as having the best targeting properties for cancer cells. The *in vivo* study of HepA mouse models based on single-photon emission computed tomography (SPECT) also showed good tumor-targeting properties of PRTH-2 labeled with ^{125}I .

© 2010 Elsevier Ltd. All rights reserved.

1. Introduction

Biocompatible polymers, such as poly(ethylene glycol)s (PEGs), polyacrylic acids (PAAs), poly(ethylene imine)s (PEIs) and poly(amido-amine)s (PAMAMs), have attracted great attention in the field of cancer diagnosis and therapy [1–6]. The synthetic polymers can easily achieve important properties, such as enhanced permeability and retention (EPR) effects and membrane destabilizing effects. The EPR effects enable polymeric molecules to be collected in tumor tissues [7–11]. The membrane destabilizing effects can prevent polymers and loaded drug molecules from being decomposed in lysosomes. Generally, such membrane destabilizing effects could be achieved by the pH-induced conformational change of anionic carboxylate polymers [12–16] or through the proton sponge effect [17–21], although the latter has been called into question [22,23]. In addition, the synthetic polymers should be traceable during the diagnostic procedures. The most frequent method for detecting the polymers utilizes conjugates of a fluorescent dye to emit intense fluorescent light in cells or tumors. However, the method used to detect the fluorescent signals suffers from many problems *in vivo*, especially when investigating deep and absorbing tissues such as the lung, spleen or liver [24].

Radionuclide imaging has been widely applied to diagnosis and therapy [25]. In radiochemistry, tyrosine moieties can be labeled with radioactive halogens, such as ^{18}F , ^{123}I , ^{125}I , and ^{131}I for posi-

tron emission tomography (PET), single-photon emission computed tomography (SPECT) and high-resolution autoradiography [26–30]. It is chemically stable for the radioactive halogen reagents to be covalently labeled onto a tyrosine moiety. In addition, the amino acid tyrosine has a better biocompatibility than various molecules used as ligands for radioactive metal ions. Therefore, it is attractive to introduce tyrosine moieties into the polymer side chains to combine the advantages of functional polymers and isotopic diagnosis.

In this paper, copolymers containing both rhodamine chromophores and tyrosine segments (PRTHs, see Scheme 1) were synthesized for the purpose of targeting cancer cells. At the same time, another copolymer without tyrosine segments (PRH) was synthesized for comparison. The rhodamine segments enabled the copolymer to be detected by fluorescence analysis, and the tyrosine segments were introduced for labeling radioactive ^{125}I for SPECT. Both PRTHs and PRH have properties that allow them to target cancer cells. The *in vitro* and *in vivo* studies verified the cancer cell targeting properties and tumor tissue targeting properties of PRTH, respectively. The copolymer PRTH would be potentially applicable for *in vivo* cancer diagnosis and therapy.

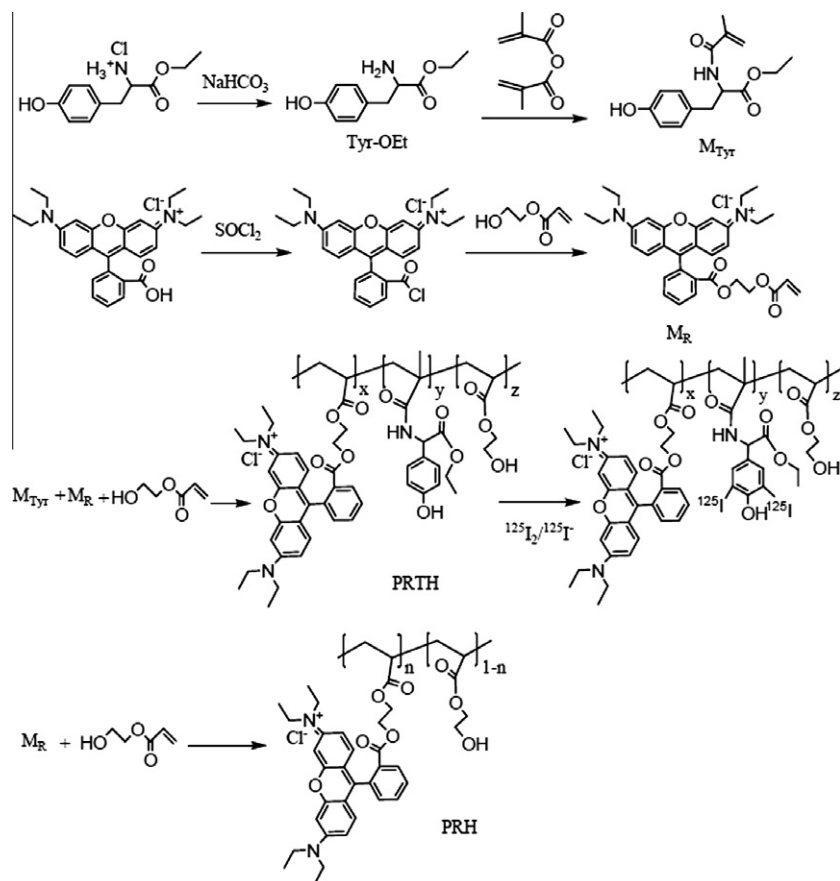
2. Experimental

2.1. Materials

2-Hydroxyethyl acrylate (HEA) was purchased from Aldrich and purified twice by passing it through a column filled with basic

* Corresponding authors. Tel./fax: +86 512 65880367 (N. Li), Tel./fax: +86 512 65882875 (J. Lu).

E-mail addresses: linajun@suda.edu.cn (N. Li), lujm@suda.edu.cn (J. Lu).



Scheme 1. Synthetic routes of PRTH and PRH.

alumina to remove the inhibitor. The initiator 2,2'-azobis(isobutyronitrile) (AIBN, A.R.) was purified by recrystallization with methanol. Rhodamine B (A.R.), thionyl chloride (A.R.), methacrylic anhydride, L-tyrosine ethyl ester hydrochloride, chloramine-T and $\text{Na}_2\text{S}_2\text{O}_5$ were purchased from Sinopharm Chemical Reagent Co., Ltd. NaI-125 was provided by the Jiangsu Institute of Nuclear Medicine. The copolymer PRH was synthesized in our lab. All other reagents and solvents were purchased from commercial sources and used as received. Bovine Calf Serum (BCS) and FCS-RPMI-1640 solution were purchased from Gibco and used as received. The BEL-7402 liver cancer cells and L-02 human normal liver cells were purchased from the Chinese Academy of Sciences Cell Bank. The liver cancer HepA mouse models and pellto-barbitalum natricum were provided by the Jiangsu Institute of Nuclear Medicine.

2.2. Characterizations

^1H NMR spectra were measured by an INOVA 400 MHz NMR spectrometer using CDCl_3 or $\text{DMSO}-d_6$ as solvents at ambient temperature. Elemental analysis was performed by an Italian 1106 FT analyzer. The molecular weights and polydispersity of the copolymers were measured using Waters 1515 Gel Permeation Chromatography (GPC) with DMF as the mobile phase at a flow rate of 1 mL min^{-1} and a column temperature of $30\text{ }^\circ\text{C}$. The size distribution values of the polymer aggregates were obtained on an Hpps501-high performance particle size analyzer. The morphology examination of the PRTH aggregates was performed on a Philips CM120 transmission electron microscope (TEM) with an accelerating voltage of 100 kV. The sample was prepared by placing a drop of the 0.2 mg mL^{-1} PRTH solution onto a mesh copper grid and drying the sample in air before measurement. The cell images were

obtained by using a Panasonic DMC-FX30 camera on an Olympus fluorescence microscope with an exposure time of 2.5 s. The images of the HepA mouse models were obtained using Philips Skylight single-photon emission computed tomography (SPECT).

2.3. Cellular uptake and imaging

The cells were incubated in a FCS-RPMI-1640 solution containing 10% BCS at $37 \pm 0.5\text{ }^\circ\text{C}$ for 25 h to obtain a 70% cell climbing ratio. The media was changed to 200 μL of 1640 solution, and PRTH or PRH was added into the cell culture to obtain a definite final concentration. The cells were incubated for 30 min at $37\text{ }^\circ\text{C}$ unless otherwise stated. The fluorescence images of BEL-7402 liver cancer cells and L-02 human normal liver cells were obtained by using a Panasonic DMC-FX30 camera on an Olympus fluorescence microscope with an exposure time of 2.5 s.

2.4. In vivo experiments

The HepA liver cancer cells were inoculated into the abdominal cavity of a normal mouse. The ascitic fluid was extracted and diluted by physiological saline to obtain the cancer cell concentration of $1 \times 10^8\text{ mL}^{-1}$. Then 0.2 mL of cancer cell solution was inoculated into the left axillary of ICR mice. Tumor tissues with a diameter of about 0.5 cm were obtained after 6 days. The HepA mouse models obtained were used in this study to investigate the accumulation behavior of PRTH in tumor tissues. PRTH-2 labeled with ^{125}I was dissolved in saline water and diluted to a concentration of 100 μCi . The PRTH-2 solution was injected through the tail vein at a dosage of 0.2 mL of solution per mouse. After the experiment, the mice were anesthetized via injection of pellto-

barbitalum natricum. The images were obtained on a Skylight SPECT.

2.5. Synthesis

2.5.1. Rhodamine B (2-hydroxyethyl acrylate) ester (M_R)

Rhodamine B (2.1 mmol) was dissolved in 1,2-dichloroethane (15 mL), then thionyl chloride (12.7 mmol) was added slowly at room temperature. The reaction mixture was refluxed for 8 h. After evaporation of the solvent in a vacuum to obtain rhodamine B acid chloride, 2-hydroxyethyl acrylate (9.6 mmol) was added dropwise to the rhodamine B acid chloride solution in dichloromethane and stirred for 24 h at room temperature. The crude product was purified by column chromatography ($\text{CH}_2\text{Cl}_2/\text{MeOH} = 30/1$, v/v) to obtain 0.9 mmol of product M_R (yield; 42.9%). ^1H NMR (CDCl_3): $\delta = 8.31$ (d, 1H, $J = 7.8$ Hz), 7.84 (t, 1H, $J = 7.5$ Hz), 7.76 (t, 1H, $J = 7.7$ Hz), 7.32 (d, 1H, $J = 7.4$ Hz), 7.08 (d, 2H, $J = 9.5$ Hz), 6.93 (d, 2H, $J = 9.5$ Hz), 6.81 (s, 2H), 6.38 (d, 1H, $J = 17.3$ Hz), 6.05 (m, 1H), 5.87 (d, 1H, $J = 10.4$ Hz), 4.29 (m, 2H), 4.17 (m, 2H), 3.66 (q, 8H, $J = 7.2$ Hz), 1.34 (t, 12H, $J = 7.1$ Hz). Anal. calcd. for $\text{C}_{33}\text{H}_{37}\text{ClN}_2\text{O}_5$: C 68.68, H 6.46, N 4.85. Found: C 68.47, H 6.31, N 4.81.

2.5.2. Ethyl 2-amino-3-(4-hydroxyphenyl)propanoate (Tyr-OEt)

L-Tyrosine ethyl ester hydrochloride (11.4 mmol) and NaHCO_3 (5.0 g) were added in water (75 mL). Dichloromethane (50 mL) was slowly added into the suspension and stirred slowly for 4 h. The dichloromethane solution was separated and evaporated to obtain a yellow solid. The crude product was washed by ethyl ether to obtain 9.1 mmol of Tyr-OEt (yield; 79.8%). ^1H NMR (CDCl_3): $\delta = 9.15$ (s, 1H), 6.95 (d, 1H, $J = 8.2$ Hz), 6.65 (d, 1H, $J = 8.4$ Hz), 4.01 (q, 1H, $J = 7.1$ Hz), 3.46 (m, 1H), 2.70 (m, 1H), 1.70 (m, 1H), 1.12 (t, 1H, $J = 7.1$ Hz). Anal. calcd. for $\text{C}_{11}\text{H}_{15}\text{NO}_3$: C 63.14, H 7.23, N 6.69. Found: C 63.06, H 7.25, N 6.63.

2.5.3. Ethyl 3-(4-hydroxyphenyl)-2-(methacrylamido) propanoate (M_{Tyr})

Tyr-OEt (7.2 mmol) and triethylamine (7.9 mmol) were dissolved in dichloromethane (40 mL). The methacrylic anhydride (7.8 mmol) in dichloromethane (40 mL) was added, and the solution was stirred at 0 °C for 24 h. After reaction, the solution was washed with NaHCO_3 (0.06 g mL^{-1}) solution and NaH_2PO_4 (0.06 g mL^{-1}) solution. The dichloromethane solution was separated and evaporated to obtain a yellow oil. The crude product was dissolved in tetrahydrofuran (THF, 10 mL). The solution was then added dropwise into water to obtain 6.1 mmol M_{Tyr} yellow oil (yield; 84.7%). ^1H NMR (CDCl_3): $\delta = 9.24$ (m, 1H), 8.19 (d, 1H, $J = 7.7$ Hz), 7.02 (m, 1H), 6.64 (m, 1H), 5.63 (m, 1H), 5.35 (m, 1H), 4.36 (dd, 1H, $J = 8.3$ Hz, $J = 14.5$ Hz), 4.05 (m, 1H), 2.90 (m, 1H), 1.79 (m, 1H), 1.12 (t, 1H, $J = 7.1$ Hz). Anal. calcd. for $\text{C}_{15}\text{H}_{19}\text{NO}_3$: C 64.97, H 6.91, N 5.05. Found: C 64.74, H 6.89, N 4.98.

2.5.4. Copoly-(M_R - M_{Tyr} -HEA) (PRTH) and copoly-(M_R -HEA) (PRH)

To prepare PRTH, M_{Tyr} , M_R , HEA and AIBN were dissolved in cyclohexanone with the mole ratio summarized in Table 1. The solution was degassed using dry nitrogen and stirred at 70 °C for

5 h. The reaction mixture was added dropwise into dichloromethane with stirring to precipitate the copolymer. The copolymer was purified with a Soxhlet extractor for 14 days and dried in vacuum at room temperature to a constant weight. In comparison, PRH was copolymerized using the same procedure above without the M_{Tyr} monomer.

2.6. Radiochemistry

PRTH-2 (25 μg) was dissolved in 25 μL of phosphate buffer (PB, 0.2 mol L^{-1} , pH = 8.0) and then 3 μL of NaI-125 (1 mCi) and 10 μL of chloramine-T (3 mg mL^{-1}) were added to the mixture, which was shaken for 1 min. $\text{Na}_2\text{S}_2\text{O}_5$ (20 μL , 5 mg mL^{-1}) was added, and mixture was shaken for an additional 3 min. The solution was diluted with 200 μL of PB solution and purified by passing through a PD10 (Sephadex G25) column to obtain ^{125}I -labeled PRTH-2.

3. Results and discussion

3.1. Characterization of PRTH

A typical ^1H NMR spectrum of PRTH-1 is shown in Fig. 1. The resonant signal at $\delta = 4.01$ ppm is assigned to the methylene protons in the hydroxyethyl segments, and the chemical shift at $\delta = 9.17$ ppm is the characteristic signal of phenolic hydroxy protons in the tyrosine segments. The content of the tyrosine segments in PRTH can be calculated from the integral area ratio of the peaks at $\delta = 9.17$ and 4.01 ppm [31]. Because the integral area of the rhodamine segments is too small to accurately calculate its content in the copolymer chain, it should be determined by using the UV-Vis absorption of the M_R monomer as a Ref. [32]. First, the standard ethanol solutions of M_R were tested to obtain the standard linear curve of absorption intensity (I_{abs} , A.U.) versus concentration (C_{MR} , $\times 10^{-6}$ mmol mL^{-1}): $I_{\text{abs}} = 0.0134 \times C_{\text{MR}} - 0.0552$. Then, the concentration of rhodamine segments in the 0.2 mg mL^{-1} ethanol solution of PRTH or PRH was tested, and the content of rhodamine segments in PRTH or PRH was calculated (see Table 1). The number-average molecular weight and polydispersity index (PDI) of PRTH and PRH were determined by GPC and are summarized in Table 1.

Fig. 2 shows the diameter distribution of PRTH aggregates in water solution. The average diameters of PRTH-1, PRTH-2 and PRTH-3 aggregates are 66 nm, 191 nm and 137 nm, respectively. It can be seen that the aggregates acquire a spherical morphology. Because the tyrosine segments are hydrophobic, PRTH containing hydrophobic and hydrophilic segments could form micelles or

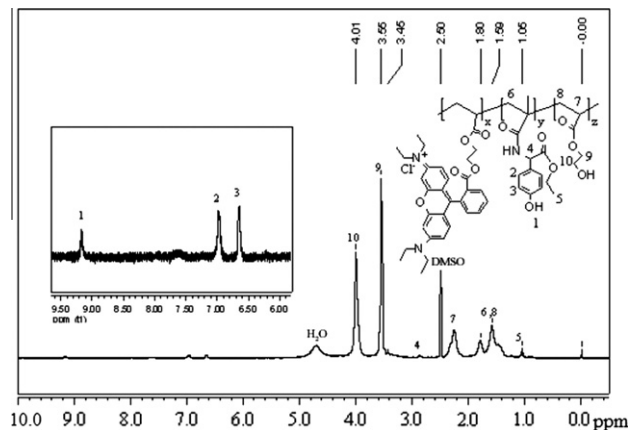


Fig. 1. ^1H NMR ($\text{DMSO}-d_6$) spectra of PRTH-1.

Table 1
The characterization data of PRTHs.

Samples	Reactant mol ratio HEA/ M_R / M_{Tyr} /AIBN	Composition [HEA]/ $[M_R]$ / $[M_{\text{Tyr}}]$	M_n	Polydispersity index (PDI)
PRTH-1	100:1:5:1	97.94%:0.15%:1.91%	25,100	2.6
PRTH-2	100:1:5:2	98.14%:0.15%:1.71%	38,800	3.6
PRTH-3	100:1:5:5	98.23%:0.14%:1.63%	31,300	2.5
PRH	100:1:0:1	99.67%:0.33%:0%	23,700	2.7

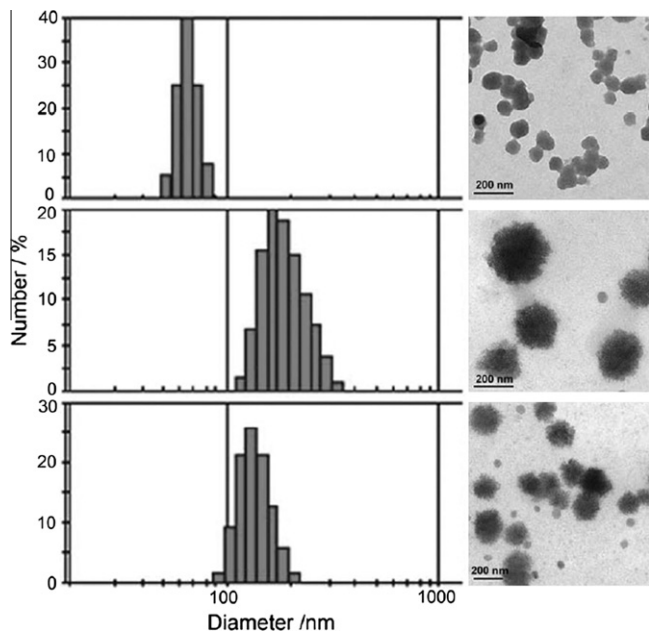


Fig. 2. Diameter distributions and TEM images (the inserted scale span is 200 nm) of PRTHs in water solution (0.2 mg mL^{-1}).

micelle-like aggregates in water solution. The reason for the different sizes of PRTH aggregates should be attributed to the different average molecular weights of each polymer because the composition of PRTHs is similar from polymer to polymer.

3.2. Cell culture studies

Fig. 3 shows the images of PRH and PRTH internalized by BEL-7402 liver cancer cells and L-02 human normal liver cells. Fig. 4 reveals the degree of cancer cell targeting properties, which were valued by comparing the fluorescent intensity of BEL-7402 with L-02 cells (I_{7402}/I_{L-02}). A high I_{7402}/I_{L-02} value means a high cancer cell targeting degree. Both PRH and PRTH can target BEL-7402 cancer cells. The values of I_{7402}/I_{L-02} in Fig. 4 reveal that the cancer cell targeting degrees are in the sequence of PRTH-2 > PRTH-3 > PRTH-1, which coincides with the sequence of the average diameters of PRTH aggregates in water (Fig. 2). The results indicate that the size

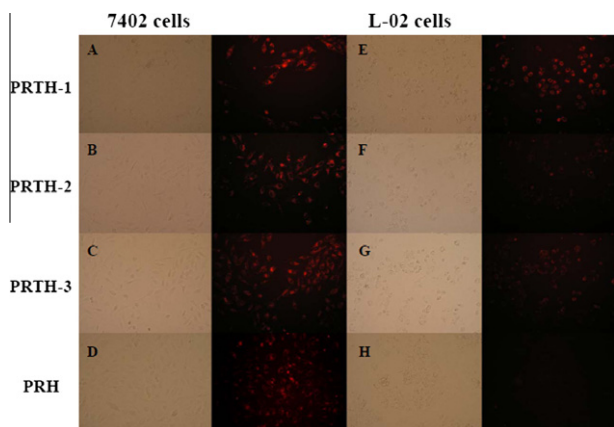


Fig. 3. Images of BEL-7402 and L-02 cells. The BEL-7402 cells were incubated in 1640 solution containing $100 \mu\text{g mL}^{-1}$ PRTH-1 (A), PRTH-2 (B), PRTH-3 (C) and PRH (D), for 30 min. The L-02 cells were incubated in 1640 solution containing $100 \mu\text{g mL}^{-1}$ PRTH-1 (E), PRTH-2 (F), PRTH-3 (G) and PRH (H).

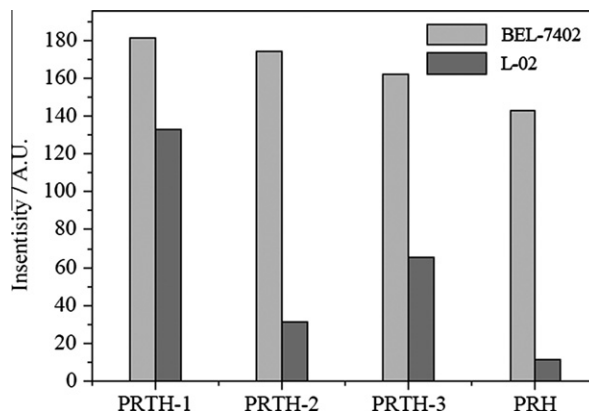


Fig. 4. Average fluorescent intensity in the BEL-7402 and L-02 cells images. I_{7402} and I_{L-02} are the average fluorescent intensity in 7402 cells and L-02 cells, respectively.

of PRTH aggregates might be correlated to their cancer cell targeting degree.

In regards to the cellular internalization mechanism of the polymers, endocytosis is considered to be the general entry mechanism. Endocytosis belongs to the energy-dependent uptake, which would be hindered at a low temperature [33]. As shown in Fig. 5, a significant reduction in cellular uptake at $4 \text{ }^\circ\text{C}$ for PRTH-2 was observed. This result indicates endocytosis to be the internalization mechanism for the uptake of PRTH. It has been previously reported that some synthetic polymers without special recognition units on main or side chains can be taken up by cells, mainly by fluid-phase or adsorptive endocytosis [34], and can further target the cancer cells [35]. However, no systematic studies have been found so far to clarify the details of the mechanism for the uptake of conjugates without receptor-specific recognition units. This mechanism should be studied further.

3.3. In vivo studies

Although PRH can target BEL-7402 cancer cells, the optical imaging diagnosis method based on detecting the fluorescent signals of PRH passing through the tissues suffers some problems *in vivo*. Similar to other optical imaging methods, fluorescence imaging is hampered by surface reflectance, absorption, scattering and autofluorescence [24]. The fluorescent signals are affected by the thickness and optical properties of the tissues. These disadvantages limit the applications of PRH. On the other hand, radionuclide imaging, which is commonly devised into two general modalities, such as SPECT and positron emission tomography (PET), can overcome these problems and has already been widely used. Tyrosine

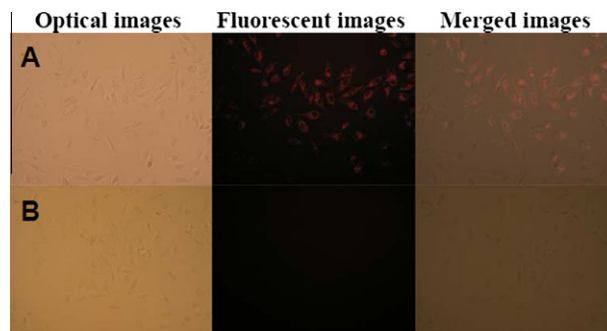


Fig. 5. Optical, fluorescent and merged images of 7402 cells incubated in 1640 solution containing $200 \mu\text{g mL}^{-1}$ PRTH-2 at $37 \text{ }^\circ\text{C}$ (A) and $4 \text{ }^\circ\text{C}$ (B).

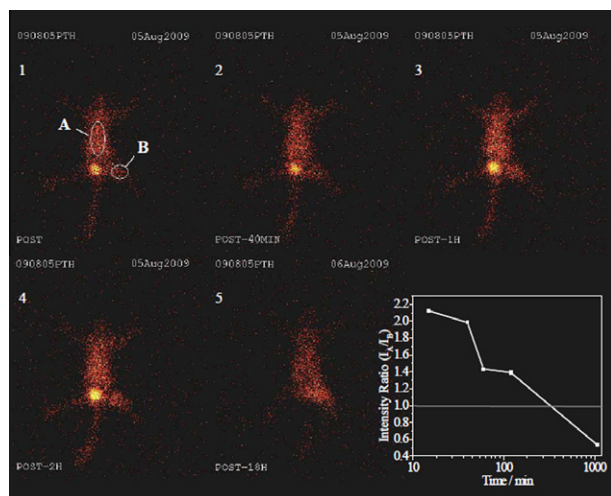


Fig. 6. SPECT images of the HepA mouse model. The site of viscera tissues was labeled A, while the site of tumor tissue was labeled B. I_A and I_B are the average radioactive intensity in the areas marked A and B, respectively. The intensity ratio is calculated by I_A/I_B .

segments were introduced for labeling radioactive halogens, such as ^{125}I , and the availability of PRTHs used *in vivo* was also examined. Fig. 6 indicates the tumor-targeting properties of PRTH-2 *in vivo* by SPECT. PRTH-2 was labeled with ^{125}I and was then injected through the tail vein of one HepA mouse model. The intensity of the radioactive signal reveals the accumulation degree of PRTH-2. The ^{125}I signal is generally enhanced in the tumor tissue marked B, while the signal decreases in the visceral tissues. The single intensity ratio of I_A/I_B clearly reveals this trend. The radioactive signal in the tumor tissue was found to be the strongest in the body ($I_A/I_B < 1$). It indicates that PRTH-2 can effectively target HepA tumor tissue. This is considered to be a result from the leaky tumor vasculature and the EPR effect of PRTH.

4. Conclusion

In summary, we have developed a novel cancer-targetable PRTH copolymer containing rhodamine and tyrosine segments. The rhodamine segments enable PRTH to be traced by fluorescent signals. However, many obstacles limit the application of the methods based on the detection of fluorescent signals. Tyrosine segments were introduced to label radioactive halogens, such as ^{125}I , for isotope detection. The BEL-7402 cancer cell targeting degree of PRTH is related to the size of the micelle-like aggregates formed in aqueous solution. The *in vivo* studies prove the ability of PRTH to target some tumor tissues and also reveal the availability of ^{125}I -labeled PRTH in SPECT. Therefore, PRTH can be detected by both fluorescent signals and radioactive signals, and it is a potential candidate in the field of *in vitro* and *in vivo* cancer diagnosis and therapy.

Acknowledgements

This work is supported by the National Natural Science Foundation of China (20876101, 20902065), the Project of Ministry of Education (20070285003), the project supported by the Major Fundamental Research Program of the Natural Science Foundation of Jiangsu Higher Education Institutions (08KJA430004) and the Innovative Research Team of Advanced Chemical and Biological Materials, Suzhou University.

References

- [1] Y. Hayashi, J.M. Harris, A.S. Hoffman, *React. Funct. Polym.* 67 (2007) 1330.
- [2] B. Mu, P. Liu, Q. Pu, *React. Funct. Polym.* 70 (2010) 578.
- [3] A. Schallon, V. Jérôme, A. Walther, C.V. Synatschke, A.H.E. Müller, R. Freitag, *React. Funct. Polym.* 70 (2010) 1.
- [4] S. Çakmak, M. Gümüşderelioğlu, A. Denizli, *React. Funct. Polym.* 69 (2009) 586.
- [5] M. Oishi, Y. Nagasaki, *React. Funct. Polym.* 67 (2007) 1311.
- [6] V. Šubr, K. Ulbrich, *React. Funct. Polym.* 66 (2006) 1525.
- [7] Y. Matsumura, H. Maeda, *Cancer Res.* 46 (1986) 6387.
- [8] H. Maeda, *Adv. Enzyme. Regul.* 41 (2001) 189.
- [9] K. Park, G.Y. Lee, Y.S. Kim, M. Yu, R.W. Park, I.S. Kim, S.Y. Kim, Y. Byun, *J. Control. Release* 114 (2006) 300.
- [10] M.K. Yu, D.Y. Lee, Y.S. Kim, K. Park, S.A. Park, D.H. Son, G.Y. Lee, J.H. Nam, S.Y. Kim, I.S. Kim, R.W. Park, Y. Byun, *Pharm. Res.* 24 (2007) 705.
- [11] E.I. Altinoğlu, T.J. Russin, J.M. Kaiser, B.M. Barth, P.C. Eklund, M. Kester, J.H. Adair, *ACS Nano* 2 (2008) 2075.
- [12] M.A. Yessine, *Adv. Drug. Deliver. Rev.* 56 (2004) 999.
- [13] M.A. Yessine, M. Lafleur, C. Meier, H.U. Petereit, J.C. Leroux, *BBA-Biomembranes* 1613 (2003) 28.
- [14] M.A. Yessine, C. Meier, H.U. Petereit, J.C. Leroux, *Eur. J. Pharm. Biopharm.* 63 (2006) 1.
- [15] S. Grube, U. Wolfrum, P. Langguth, *Biomacromolecules* 9 (2008) 1398.
- [16] S. Flanary, A.S. Hoffman, P.S. Stayton, *Bioconjugate Chem.* 20 (2009) 241.
- [17] A. San Juan, D. Letourneur, V.A. Izumrudov, *Bioconjugate Chem.* 18 (2007) 922.
- [18] H.W. Duan, S.M. Nie, *J. Am. Chem. Soc.* 129 (2007) 3333.
- [19] Y. Hu, T. Litwin, A.R. Nagaraja, B. Kwong, J. Katz, N. Watson, D.J. Irvine, *Nano Lett* 7 (2007) 3056.
- [20] A. Zintchenko, A. Philipp, A. Dehshahri, E. Wagner, *Bioconjugate Chem.* 19 (2008) 1448.
- [21] M.L. Patil, M. Zhang, O. Taratula, O.B. Garbuzenko, H. He, T. Minko, *Biomacromolecules* 10 (2009) 258.
- [22] P. Dubruel, B. Christiaens, M. Rosseneu, J. Vandekerckhove, J. Grooten, V. Goossens, E. Schacht, *Biomacromolecules* 5 (2004) 379.
- [23] A.M. Funhoff, C.F. van Nostrum, G.A. Koning, N.M.E. Schuurmans-Nieuwenbroek, D.J.A. Crommelin, W.E. Hennink, *Biomacromolecules* 5 (2004) 32.
- [24] S. Dufort, L. Sancey, C. Wenk, V. Jossierand, J.L. Coll, *BBA-Biomembranes* 1798 (2010) 2266.
- [25] H. Zaidi, H. Veas, M. Wissmeyer, *Acad. Radiol.* 16 (2009) 1108.
- [26] M. Zuhayra, A. Alfteimi, C.V. Forstner, U. Lützen, B. Meller, E. Henze, *Bioorgan. Med. Chem.* 17 (2009) 7441.
- [27] N. Shikano, Y. Kanai, K. Kawai, N. Ishikawa, H. Endou, *Nucl. Med. Biol.* 30 (2003) 31.
- [28] N. Shikano, M. Ogura, H. Okudaira, S. Nakajima, T. Kotani, M. Kobayashi, S. Nakazawa, T. Baba, N. Yamaguchi, N. Kubota, Y. Iwamura, K. Kawai, *Nucl. Med. Biol.* 37 (2010) 197.
- [29] O. Prante, J.T. Deichen, C. Hocke, T. Kuwert, *Nucl. Med. Biol.* 31 (2004) 365.
- [30] B. Kühnast, F. Dollé, S. Terrazzino, B. Rousseau, C. Loc'h, F. Vaufrey, F. Hinnen, I. Doignon, F. Pillon, C. David, C. Crouzel, B. Tavitian, *Bioconjugate Chem.* 11 (2000) 627.
- [31] B. Xu, J. Yuan, T. Ding, Q. Gao, *Polym. Bull. (Electronic)* (2009) 1436.
- [32] H. Tian, Y. He, C. Chang, *J. Mater. Chem.* 10 (2000) 2049.
- [33] N.W.S. Kam, Z. Liu, H.J. Dai, *Angew. Chem.* (2006) 591.
- [34] J. Callahan, J. Kopeček, *Biomacromolecules* 7 (2006) 2347.
- [35] F. Hudecz, J. Reményi, R. Szabó, G. Kóczán, G. Mez, P. Kovács, D. Gaál, *J. Mol. Recognit.* 16 (2003) 288.